Rohman, H.N., Hayashida, T., & Hara, T. (2025), Site effect study using strong motion record of 2022 Cianjur earthquake and surrounding earthquakes, Synopsis of IISEE-GRIPS Master's Thesis, Bulletin of IISEE, 62

SITE EFFECT STUDY USING STRONG MOTION RECORD OF 2022 CIANJUR EARTHQUAKE AND SURROUNDING EARTHQUAKES

Hadi Nur ROHMAN[1]

Supervisors: Takumi HAYASHIDA[2]**, Tatsuhiko HARA**[2]

ABSTRACT

Understanding site effects is important for assessing seismic hazards as part of a disaster mitigation effort. However, site effect studies in Indonesia remain limited despite the increasing availability of ground motion records. This study aims to evaluate the characteristics of site effects using strong-motion data in Indonesia and to examine their influence on earthquake damage. We applied the Generalized Inversion Technique (GIT), using an event assumed to follow the ω^{-2} source model as a reference. Ground motion records from mainshock and aftershocks of the 2022 Cianjur earthquake (Mw5.6), along with several surrounding events, were used to estimate site effects in and around the affected area. GIT was first applied using only the accelerometer records and then using all available data, including seismic intensity meters with MEMS sensors. The estimated site effects from both datasets showed little differences at accelerometer stations, indicating that the difference in sensor types does not affect the stability of the inversion. Amplitudes of site effects at intensity meter stations tend to be higher than those at accelerometer stations, possibly because intensity meters were located in areas with high amplification. Differences in the reliable frequency ranges were also observed due to differences in sensor characteristics. A comparative analysis with damaged house ratios revealed moderate to strong correlations, especially at frequencies around 1 Hz, suggesting that ground motions near this frequency band may have contributed to the observed damage.

Keywords: Site effect, Strong-motion records, Generalized Inversion Technique, Cianjur Earthquake.

1. INTRODUCTION

The volume of seismic data in Indonesia has been increasing along with the high seismic activity and the development of seismic observation networks. This increase in data provides an opportunity for researchers to conduct earthquake analyses and seismic hazard studies. Although many studies have been conducted using seismic data, the utilization of the BMKG strong-motion data requires improvement and optimization. BMKG's strong-motion records are mainly used to generate ShakeMap and support the earthquake early warning system. For disaster mitigation, the study of seismic wave characteristics is one of the important approaches since seismic recordings contain information on earthquake sources, propagation paths, and site effects.

On November 21, 2022, at 06:21 UTC, a devastating earthquake with a moment magnitude (Mw) of 5.6 struck Cianjur Regency, West Java, Indonesia. Although its magnitude was not too large, the earthquake caused significant damage. Recent studies suggest that the unidentified faults contributed to the event (Arwasaputra et al., 2024; Supendi et al., 2023). The tectonic and geological conditions indicate that Cianjur is vulnerable to earthquakes; thus, subsurface structural analysis is necessary (Pangestu et al., 2025) through site amplification studies, to better understand local seismic response and support efforts in earthquake risk mitigation in this area.

[1] Meteorological, Climatological, and Geophysical Agency (BMKG), Indonesia.
[2] International Institute of Seismology and Earthquake Engineering (IISEE), Building Research Institute (BRI).

Approved as Master Paper of DMP by BRI/GRIPS

This study aims to quantify site effects in the Cianjur area and its surroundings using seismic observation data. This study applied the Generalized Inversion Technique (GIT), following the approach of Moya & Irikura (2003), focusing on the influence of different sensor types: accelerometers and seismic intensity meters equipped with MEMS sensors. In addition, the estimated site amplification factors were compared with other indicators of site amplification, including the earthquake horizontal-to-vertical spectral ratio (EHVSR) and Vs30, to examine their interrelationships and to assess the contribution of site effects to the observed earthquake damage.

2. METHODOLOGY

2.1. GIT

As an early work of GIT, Andrews (1986) assumed that the power spectrum of observed ground motion recording is the product of the station-response and source power spectrum. Iwata and Irikura (1988) incorporated inelastic losses of seismic wave energy as the path term, which they expressed using the quality factor (Q-value). One of the advantages of GIT is its ability to separate the source (*S*), path (*P*), and site effect (*G*). In the frequency domain, the observed spectrum of the *i*-th earthquake at the *j*-th station $O_{ij}(f)$ is described as the product of the source spectrum of the *i*-th earthquake $S_i(f)$, the path effect $P_{ij}(f)$, and the site effect at the *j*-th station $G_j(f)$:

$$O_{ij}(f) = S_i(f)\, P_{ij}(f)\, G_j(f), \tag{1}$$

The path effect $P_{ij}\ (f)$ contains both the geometrical spreading effect and inelastic attenuation related to energy dissipation. Assuming a point-source model, the path effect can be written as follows:

$$P_{ij}(f) = {R_{ij}}^{-1}\ e^{\frac{-\pi f R_{ij}}{Q(f)\beta}}, \tag{2}$$

where R_{ij} is the hypocentral distance from the *i*-th event to the *j*-th station, $Q\ (f)$ is the frequency-dependent quality factor, and β is the average shear-wave velocity along the path.

For the analysis, we used a GIT software package developed by Dr. T. Hayashida (International Institute of Seismology and Earthquake Engineering), based on the method of Moya & Irikura (2003). The package consists of four Fortran programs. The first program extracts spectral files from the S-waves portions with a window of 20.48 seconds. The data were filtered using the following criteria: amplitude range of 0.2–50 cm/s^2, hypocentral distance range of 5–150 km, depth range of 3–35 km, and minimum magnitude of 3. We also performed Fast Fourier Transform (FFT) to obtain the Fourier Spectrum in the horizontal component and the earthquake horizontal-to-vertical spectral ratio (EHVSR) for the S-wave portion. The second program constructs matrices for the inversion. The third program estimates the corner frequency of the reference events by selecting pairs of large and small events. These events are assumed to follow the ω^{-2} source model (Brune, 1970). The fourth program incorporates these reference events as constraints in the inversion. Finally, the site effect, *Q*-values, and source spectrum were estimated using linear inversion.

3. DATA

We used earthquake parameters around Cianjur area from the BMKG catalog, from 2022 to 2023. We then selected earthquakes that met the following criteria: a magnitude range of 3–5.6, a depth between 3–60 km, and a focus area between 6.35–7.35 S and 106.6–107.5 E. This range is important to keep regional homogeneity and avoid the domination of the path effect. Based on these criteria, 52 events were selected, including the main shock, as shown in Figure 1.

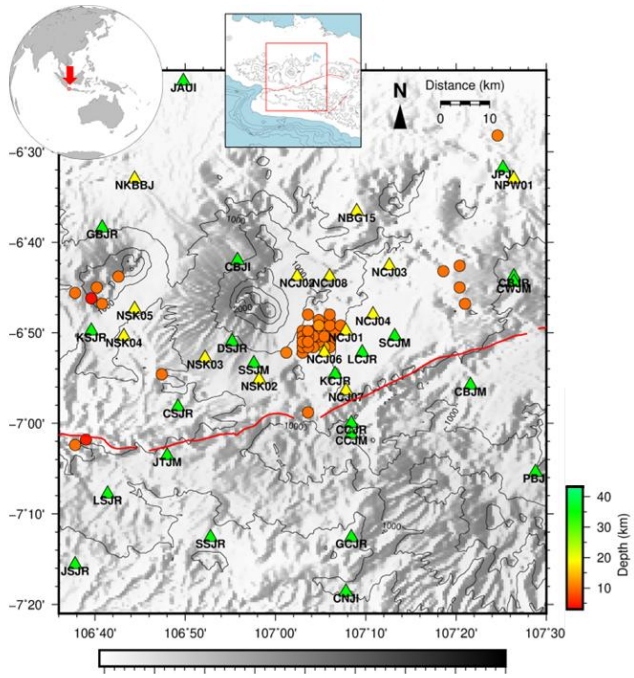

Figure 1. The study area. Circles denote the distribution of events with depth variation. The thick red curve shows the active fault.

We utilized ground motion data recorded by the BMKG strong-motion station network located in the Cianjur area. The data were provided in miniSEED format, and we selected 1,353 strong-motion recordings for our analysis. Our dataset includes two types of instruments: accelerometers and seismic intensity meters.

The sensor types used in this study are summarized in Table 1. For the seismic intensity meters, we specifically selected only the (P-alert +) sensor type, which featured a three-component MEMS sensor. The locations of these stations are shown in Figure 1. In total, we used data from 23 accelerometer stations and 14 seismic intensity meter stations, represented by green and yellow triangles, respectively.

Zero baseline correction and conversion to (.dat) format was performed on all miniSEED data. For the seismic intensity meter data, a correction factor of $1 / 1671.8^2$ was applied to match the amplitude units with the accelerometer data in cm/s².

Table 1. The sensor type of the BMKG strong-motion network in this study.

No	Type	Sensor	Nmbr Station	Sampling	Sensitivity (count/g)	Digitizer Resolution	Range of Output
1	Accelerometer	Titan	7	100 Hz	203943.388/ 203999.898	24 bit	40 Vpp
		G210-S	12	100 Hz	279620.266	24 bit	40 Vpp
		TSA-100S	2	100 Hz	203943.388	24 bit	40 Vpp
		FBA ES-T	2	100 Hz	427692.771	24 bit	40 Vpp
2	Intensitymeter	P-Alert+	14	100 Hz	1671.8	16 bit	4g
Total Stations			37				

4. RESULTS AND DISCUSSION

4.1. Inversion result

The corner frequencies were estimated to model the source spectrum of two reference events: a larger event on November 21, 2022 (M_0: 4.68×10^{15} Nm) and a smaller event on November 28, 2022 (M_0: 8.76×10^{13} Nm). We performed two inversions using the smaller event, with a corner frequency of 2.87 Hz, as a reference to stabilize the results. The first inversion utilized only strong-motion data from accelerometer stations, while the second included all available data from both accelerometers and seismic intensity meters. The first inversion considered 51 events and 463 strong-motion records, whereas the second encompassed 52 events and 747 records. The differences between the two inversions in terms of site amplification or source spectra were minimal, indicating stability in site term estimates regardless of sensor type. Minor variations in the Q-value were noted, likely due to differences in data density and station distribution. Therefore, our discussion will focus on the results from the second inversion.

Figure 2 shows the estimated site amplification factors at (a) accelerometer stations and (b) seismic intensity meter stations. An increasing trend was observed at frequencies below 0.5 Hz at the accelerometer stations and 1 Hz at the intensity meter stations, possibly due to noise contamination. A decreasing trend was seen at frequencies above 5 Hz, likely due to wave attenuation in the propagation medium, as higher-frequency waves dissipate energy more rapidly.

We also observed that the site amplification at intensity meter stations (Figure 2(b)) tends to be higher than at accelerometer stations (Figure 2(a)). This may be due to the intensity meter station location at sites with higher amplification. It is also necessary to verify the differences in the characteristics of the instruments. Further investigation is required by placing two sensors with different characteristics at exact locations to confirm this point, which would be essential for future studies.

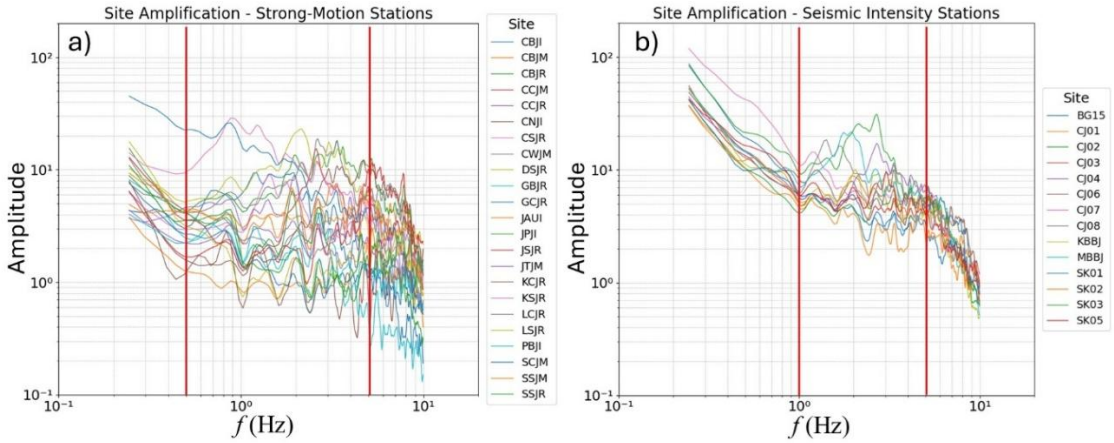

Figure 2. Site amplification values for each station in the frequency range of 0.2 Hz to 10 Hz, using event 2211280905 as a reference. The vertical red line indicates the limit of the reliable frequency range.

The estimated Q-value from this study is approximated as $Q(f) = 107.74f^{0.84}$, over the frequency range 0.2–10 Hz (Figure 3). Q-value increases with increasing frequency and shows frequency dependency. The value is close to the previous studies in Japan.

The inversion results for the source factor are shown in Figure 4. Most curves follow the ω^{-2} model. However, some curves exhibit flattening or increasing trends at higher frequencies, likely due to contamination of reflected and surface waves in the wave portion used in the analysis. On the other hand, some source spectrum values increase towards the lower frequency, which may result from low-frequency noise contamination in the original data at several stations.

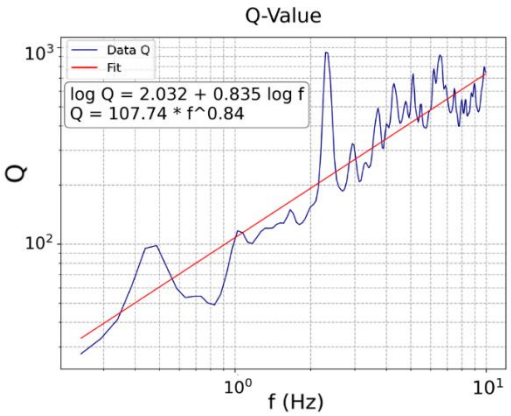

Figure 3. Estimated Q-Value.

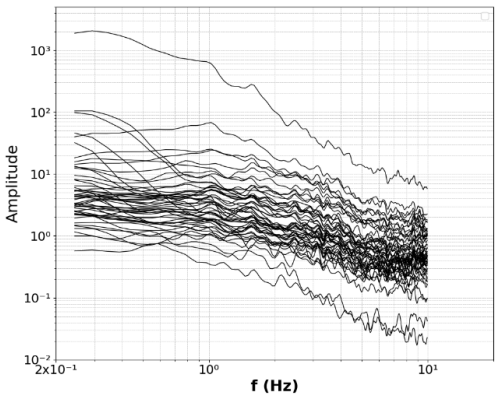

Figure 4. The inversion results for the source factor.

4.2. Comparison of site amplification factors with other indicators

We compared the estimated site amplification factors with the Earthquake Horizontal to Vertical Spectral Ratio (EHVSR). Although the absolute amplitude values from GIT and EHVSR are not directly comparable (Ito et al., 2020), their dominant frequencies generally match (Ito et al., 2020; Kawase et al., 2019). This comparison focuses on the first peak frequency as a validation indicator for the site amplification results.

Figure 5 shows a linear comparison between the EHVSR dominant frequency and the peak site amplification frequency derived from the GIT. Most stations show a good agreement, but several sites show a mismatch in dominant frequencies, which may be due to the instrumental noise.

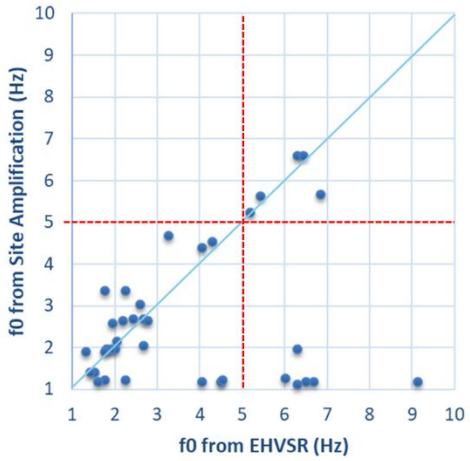

Figure 5. Comparison of dominant frequency between EHVSR and GIT.

We also examined the relationship between average site amplification and Vs30 values. Amplification values were averaged within a window of ±0.2 at frequencies 1, 2, 3, 4, and 5 Hz, and were correlated with the reciprocal Vs30 values, provided by BMKG. The results indicate a positive-moderate relationship at a 1–3 Hz with correlation coefficients of 0.37, 0.34, and 0.35, respectively. There is a low correlation (0.13) at 4Hz and a negative correlation (-0.12) at 5 Hz.

Finally, we examined how site amplification results from the GIT correlated with building damage. We utilized house damage distribution maps that are available on the BNPB website. Only six stations (CJ01, CJ02, CJ04, CJ06, CJ08, and LCJR) were located within the map and around heavily damaged areas, which coincide with the newly identified fault zone. We counted the total house damage for each site within a 1 km radius. The house damage ratio was obtained by dividing the number of slightly, moderately, and severely damaged houses by the number of total houses.

A strong correlation was found between the site amplification and damaged houses at 1 Hz, listed in Table 2. Most houses in Cianjur are low-rise buildings, which may resonate with low to medium frequencies. The observed damage in the Cianjur region may have been amplified by site effects, particularly around a frequency of 1 Hz. Further studies are required to explore the relationship between site amplification and building damage, using dense site data and varying building types.

Table 2. Correlation coefficient between site amplification and damaged house ratio.

Freq (Hz)	Correlation (r)		
	slightly	moderately	severely
1	-0.87	0.68	0.64
2	-0.31	0.56	0.08
3	-0.39	0.35	0.27
4	-0.31	0.25	0.23
5	0.11	0.50	-0.35

5. CONCLUSIONS

This study applied the GIT to separate site amplification, attenuation, and source factors using a selected reference event. This analysis focused on quantifying site amplification in the area of the 2022 Cianjur earthquake by selecting ground motion data recorded at the surrounding stations, including the mainshock data.

We performed inversions using only accelerometer station data and combined data from both accelerometers and seismic intensity meters. A comparison between the two results showed that the inversion results were stable regardless of the sensor type. However, the difference between the accelerometer station and the seismic intensity meter station was evident in the lower frequencies. The accelerometer stations provided a reliable amplification factor of up to 0.5 Hz. The seismic intensity

meter was reliable only from 1 Hz and above. We recommend the use of sensors with similar characteristics for future studies.

The comparison of dominant frequencies between EHVSR and GIT shows good agreement at most stations. A comparison of site amplification with reciprocal Vs30 showed a moderate relationship in the 1–3 Hz frequency range. Although the relationship between them is not strong, there are indications that site amplification contributes to Vs30 variation. A comparison of site amplification with damaged houses revealed a moderate to strong correlation at 1 Hz. Further studies of this correlation using denser data and varying building types are necessary.

We recognize that site effects are not the only factor influencing building damage. Other factors (e.g., source mechanisms, proximity to the epicenter, and building quality) need to be considered. Therefore, integrating site amplification with other parameters will enhance the effectiveness of earthquake disaster mitigation strategies.

ACKNOWLEDGEMENTS

This research was conducted during the individual study period of the training course "Seismology, Earthquake Engineering and Tsunami Disaster Mitigation" by the Building Research Institute, JICA, and GRIPS. I would like to express my sincere gratitude to my supervisors, Dr. Takumi Hayashida and Dr. Tatsuhiko Hara, for their valuable support and experience, which helped me to complete my research successfully, and to Dr. Eri Ito for her constructive comments on this study. I would like to express my gratitude to the Indonesian Meteorological, Climatological, and Geophysical Agency (BMKG) for providing the strong motion data and Vs30 used in this study. Additionally, I used information from damage distribution maps of affected houses, which are available on the National Disaster Management Authority (BNPB) website.

REFERENCES

Andrews, D. (1986). Objective determination of source parameters and similarity of earthquakes of different size. *Earthquake source mechanics*, *37*, 259-267.

Arwasaputra, L. T., Setiawan, M. R., Sugiarto, B., Permanasari, I. N. P., & Pardede, I. (2024). Geophysical investigation of the 2022 Cianjur earthquake: Uncovering a new active fault. E3S Web of Conferences,

Brune, J. N. (1970). Tectonic stress and the spectra of seismic shear waves from earthquakes. *Journal of geophysical research*, *75*(26), 4997-5009.

Ito, E., Nakano, K., Nagashima, F., & Kawase, H. (2020). A method to directly estimate S‐wave site amplification factor from horizontal‐to‐vertical spectral ratio of earthquakes (eHVSRs). *Bulletin of the Seismological Society of America*, *110*(6), 2892-2911.

IWATA, T., & IRIKURA, K. (1988). Source parameters of the 1983 Japan Sea earthquake sequence. *Journal of Physics of the Earth*, *36*(4), 155-184.

Kawase, H., Nagashima, F., Nakano, K., & Mori, Y. (2019). Direct evaluation of S-wave amplification factors from microtremor H/V ratios: Double empirical corrections to "Nakamura" method. *Soil Dynamics and Earthquake Engineering*, *126*, 105067.

Moya, A., & Irikura, K. (2003). Estimation of site effects and Q factor using a reference event. *Bulletin of the Seismological Society of America*, *93*(4), 1730-1745.

Pangestu, F. D., Ry, R. V., Zulfakriza, Z., & Lesmana, A. (2025). Estimation of Shear Wave Velocity (Vs) Using Earthquake Horizontal-to-Vertical Spectral Ratio (EHVSR) Method and Cianjur 2022 Aftershock Data. IOP Conference Series: Earth and Environmental Science,

Supendi, P., Winder, T., Rawlinson, N., Bacon, C. A., Palgunadi, K. H., Simanjuntak, A.,…Shiddiqi, H. A. (2023). A conjugate fault revealed by the destructive Mw 5.6 (November 21, 2022) Cianjur earthquake, West Java, Indonesia. *Journal of Asian Earth Sciences*, *257*, 105830.